Parametric Analysis of Aircraft Wing Weight Using Low-Order Physics-Based Analysis

Erik D. Olson[1]

NASA Langley Research Center, Hampton, VA 23681

Quinten Henricks[2]

The Ohio State University, Columbus, OH 43210

In the conceptual aircraft design phase, prediction of the empty weight typically relies on empirically-based regression equations which execute quickly and require little detailed information about the internal structural layout. Since they are based on existing aircraft, however, empirical methods can lose their validity for newer technologies and unconventional configurations. Designers can transition to higher-order, physics-based analysis methods to improve the accuracy of the weight prediction, but at the cost of complex model setup and increased computational time. This paper describes a methodology for low-order aero-structural analysis of conceptual aircraft configurations that increases the use of physics-based analysis in conceptual design, but is less complex and time-consuming than higher-order methods such as finite-element analysis. The methodology uses Vehicle Sketch Pad (OpenVSP) to model the aircraft geometry, and ASWING to perform the aero-structural analysis. The internal forces and moments from the ASWING analysis are post-processed to calculate the resulting direct and shear stresses in the structure, and the thickness distributions of the aircraft components are varied to match the maximum von Mises stress at each cross section to the material allowable. To offset the increased computational time relative to empirical weight equations, a process is studied which uses parametric variation to develop a regression equation relating the weight of the aircraft wing to major design variables. This new weight equation is similar to existing empirical equations, but is built using the more physics-based methodology; the new equation could be used to augment or replace portions of the empirical database to improve the validity of the wing weight prediction for unconventional configurations and advanced technologies.

I. Nomenclature

A	=	cross-sectional area
$\mathbf{b}$	=	error residual vector of spanwise loading
c, s, n	=	local chordwise, spanwise, and normal coordinates
C	=	twist influence matrix
E	=	elastic modulus
E	=	stiffness matrix
g	=	acceleration of gravity
G	=	shear modulus
F	=	internal force
i, j	=	Matrix row and column indexes
I	=	area moment of inertia
$\bar{I}$	=	area moment of inertia per unit thickness
J	=	torsion constant
k	=	iteration index
K	=	shear stiffness constant
M	=	internal moment
p	=	perimeter
P	=	internal pressure

---

[1] Aerospace Engineer, Aeronautics Systems Analysis Branch, Senior Member AIAA.
[2] Graduate Research Assistant, Student Member AIAA.

R	=	cross-sectional radius
R^2	=	coefficient of determination
S	=	wing reference area
t	=	time, thickness
t_{min}	=	minimum material gauge
u, v	=	parametric surface coordinates
$\overline{U}$	=	body velocity vector
$\overline{V}_{gust}$	=	gust velocity vector
x, y, z	=	Cartesian coordinates
$\mathbf{x}$	=	change vector for spanwise twist distribution
σ	=	direct stress
$\sigma_{allowable}$	=	maximum allowable stress
σ_v	=	von Mises stress
$\sigma_{v_{max}}$	=	maximum von Mises stress in a cross section
σ_1, σ_2	=	maximum and minimum principal stresses
τ	=	shear stress
$\overline{\Omega}$	=	body rotational velocity vector
Subscripts		
b	=	basic (open section) shear
ca	=	center of area
shell	=	value for outer shell
solid	=	value for enclosed area
TOT	=	total
0	=	closed section shear constant

II. Introduction

To calculate the mission performance of an aircraft concept, a designer must have an estimate of the empty weight of the aircraft. However, during the conceptual aircraft design phase an accurate estimate of the weight can be difficult to obtain because little detail is typically available about the internal structure and the type and size of various subsystems. Traditionally, designers have tended to rely on regression equations of available historical data for existing aircraft [1].

One tool that makes use of such empirical weight estimates is the Flight Optimization System (FLOPS)[2], which has been used extensively by government, academia, and industry for conceptual-level weight prediction, mission performance and aircraft synthesis studies. However, FLOPS was originally developed in the 1980s, and as new aircraft designs and technologies have entered the market, FLOPS has developed several shortcomings that limit its ability to produce accurate weight estimates. The FLOPS weights equations are based on conventional tube-and-wing aircraft configurations and technologies that were in service at the time the code was originally developed, so its validity for analysis of unconventional configurations and newer technologies is limited. Some modifications have been made to adapt the weights prediction to specific unconventional configurations, such as the blended wing-body[3], but other types of configurations remain a challenge. Even some state-of-the-art conventional aircraft have wing aspect ratios that are outside of FLOPS' weights database, and the code can struggle to properly estimate the sensitivity of the wing weight to even higher aspect ratios.

One approach to improving the conceptual-level analysis of unconventional configurations is to transition to the use of higher-order, physics-based methods. The advantage of a physics-based analysis is that it is more likely to directly capture the effect of design variables through physical laws, and thus may be able to better predict trends outside of the existing empirical database. On the other hand, empirical regression methods tend to run very quickly, whereas physics-based methods can take from one to many orders of magnitude longer to perform an analysis. Finite-element methodology (FEM) can capture accurate weight trends but model setup tends to be complex and time-consuming, and execution can be too computationally expensive for general use in conceptual design studies.

The goal of this study was to develop a lower-order methodology which is more physics-based than pure empirical regression equations and thus is more applicable to more modern structures and unconventional concepts—such as high-aspect-ratio wings and truss-braced wings—but does not require excessive design information or incur a prohibitive

computational cost when compared to empirical methods. For efficiency, it was desired that a methodology be built by leveraging existing tools which contain a full set of features such as flutter, full-body flexible dynamics, gust response, and time-domain calculations.

Though not as computationally expensive as a FEM, even a lower-order physics-based method will increase the computational cost of the weight estimation methodology. To overcome the increased computational time, an approach was investigated which uses parametric variation to develop new equations relating the weights of the aircraft components to major design variables. These new weights equations are similar to the existing empirical equations, but are built using the more physics-based analysis method and are presumably more applicable to designs outside the original empirical database. The new equations can be used to augment or replace portions of the empirical database to improve the validity of the weights prediction for unconventional configurations and advanced technologies.

III. Methodology

This section describes the methodology that has been developed for rapid aero-structural weight estimation of conceptual-level aircraft configurations. The methodology consists of three main functions: geometry definition, aero-structural analysis, and structural sizing.

A. Geometry Definition

In this methodology, the aircraft geometry is defined using Vehicle Sketch Pad (OpenVSP)[4], which is an open-source parametric geometry modeler that allows rapid geometry creation using high-level design parameters. OpenVSP has been used extensively for conceptual design studies of aircraft, including studies using higher-order analysis[5–7]. To facilitate multi-disciplinary and multi-fidelity analysis, OpenVSP has the ability to generate and export several *degenerate* forms of the geometry[8]. The degenerate models represent the type of abstraction required to perform low- to medium-order analysis for a range of aeronautical disciplines. Each node in the degenerate models represents a discrete point in the geometric representation; in addition, the node retains information about the aggregate properties of the full geometry. By creating these degenerate models internally, OpenVSP maintains a direct link between the "master"—i.e., analytical—geometry and the degenerate models. This way, any changes to the design are always reflected in all of the degenerate models and in the analysis methods that employ them. The degenerate models exported from OpenVSP are at four different *orders*, or levels of abstraction. These levels are, in decreasing order: Surface, Plate, Stick, and Point[8] (Fig. 1).
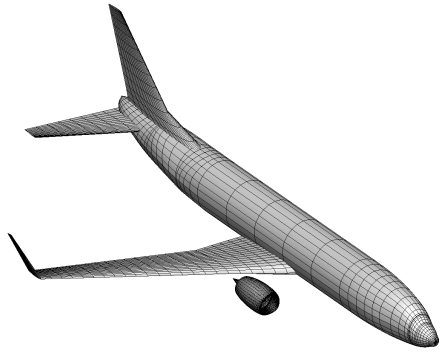
The *Degenerate Surface* (Fig. 1(a)) represents the discrete surface nodes of a component mapped against parametric *u* and *v* coordinates, and is a suitable level of abstraction for three-dimensional analysis methods, such as an aerodynamic panel method or acoustic scattering code. The nodes of the Surface model are a set of non-intersected, structured meshes for the individual components of the model (such as fuselage, wing, and tails).

The *Degenerate Plate* (Fig. 1(b)) replaces the three-dimensional surface of each component with a zero-thickness mean camber surface mapped against *u* and *v*. The Plate model is suitable for analysis methods that assume that the surface is very thin, such as an aerodynamic vortex-lattice code, an equivalent-plate structural analysis, or a planar acoustic shielding analysis.
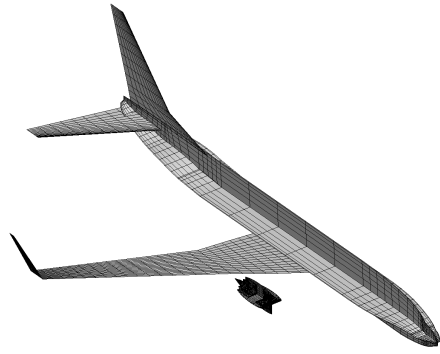
The *Degenerate Stick* (Fig. 1(c)) represents each component as a single reference line containing information about the spanwise (for lifting surfaces) or lengthwise (for bodies) properties of the component, mapped against the *u* parameter. The Stick model is suitable for aerodynamic analysis using a lifting-line code, or for structural analysis using an equivalent-beam method.

Finally, the *Degenerate Point* (Fig. 1(d)) represents each component as a single point containing information about the component as a whole. The Point model is suitable for aerodynamic analysis using empirical or semi-empirical skin-friction analysis. The Point maintains information about the surface area, volume, center of mass, and mass moments of inertia of each component.
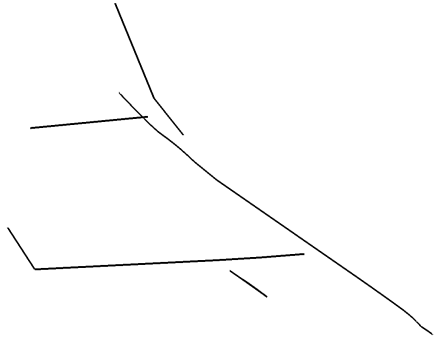
This methodology makes use of a multi-disciplinary, multi-fidelity mapping process that is built around the degenerate geometric representations exported from an OpenVSP model and was previously described in Ref. 9. This process creates a *DegenGeom* object that is instantiated by reading in and parsing a degenerate geometry file that has been exported by OpenVSP. Individual analyses are included in an analysis framework using wrappers, which are able to access previous analysis results from the DegenGeom object, pass them to the analysis method for execution, and then store the new analysis results and map them onto the degenerate models for use in subsequent analyses.

(a) Surface model

(b) Plate model

(c) Stick model

(d) Point model

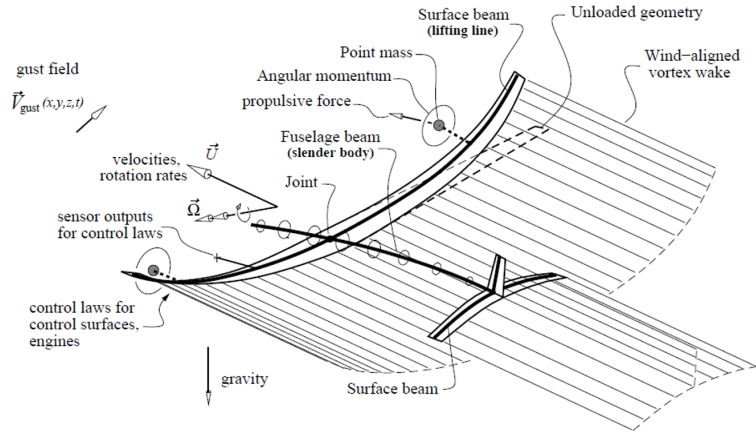**Fig. 1   OpenVSP degenerate geometric models for a tube-and-wing aircraft configuration**

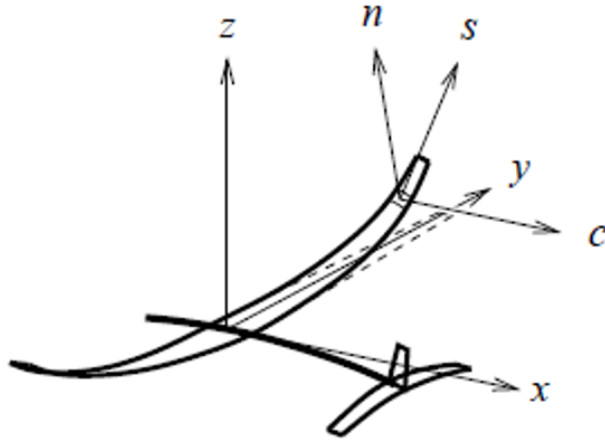**Fig. 2   Features of the ASWING program.** *Source*: **Ref. 10. Used with permission.**

Fig. 3   ASWING local coordinate definition. *Source*: **Ref. 10. Used with permission.**

B. Aero-Structural Analysis

Once the geometry has been modeled in OpenVSP and exported in its degenerate forms, the aero-structural analysis of the aircraft configuration is performed using ASWING. ASWING uses a lifting-line aerodynamic analysis coupled with a non-linear equivalent-beam structural analysis[10], and thus is able to work directly with the Stick model exported from OpenVSP. Figure 2 illustrates the full set of features available in ASWING; some capabilities such as unsteady analysis, gust response, and control-law design are not currently used in this methodology, but may be included in the future.

C. Preparation of ASWING Model

For each beam in the model, ASWING requires the stiffness properties, mass moments of inertia, center of mass, elastic axis, tension axis and sectional aerodynamics at each cross section along the length of the beam. These are defined in the local c, s, n coordinate system as shown in Fig. 3. Some of these properties are available directly from the OpenVSP model, whereas others may be derived from the OpenVSP model and augmented by additional information supplied by the user, as described below.

To define the stiffness properties of the aircraft components, ASWING requires the stiffness matrix, E, which takes
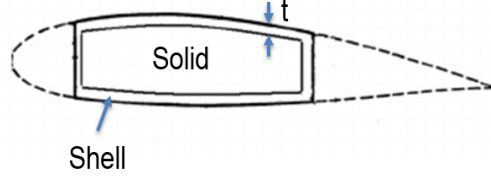
Fig. 4 Shell and solid components of a wing box cross section

the form

$$E \equiv \begin{bmatrix} (EI)_{cc} & (EI)_{cs} & (EI)_{cn} \\ \cdot & (GJ) & (EI)_{sn} \\ \cdot & \cdot & (EI)_{nn} \end{bmatrix} \tag{1}$$

The additional properties GK_c and GK_n represent the shear stiffness in the chordwise and normal axes, and EA represents the extensional stiffness. In order to build the ASWING model from the OpenVSP geometry and limit the amount of preprocessing involved, the methodology makes use of several properties of each beam that have been automatically exported to the Stick model. Each cross section of the Stick model maintains information about the properties of the *shell*, or surface contour, and the *solid*, or enclosed cross section (Fig. 4), of the original complete surface. For the outer thin-walled shell, the following properties are available for each cross section:

- the location of the center of area, $(x_{ca}, y_{ca}, z_{ca})_{shell}$,
- area moments of inertia per unit thickness, $\bar{I}_{cc}, \bar{I}_{nn}$, and $\bar{I}_{cn}$, and
- perimeter, p, of the cross section.

For each solid cross section, the following properties are available:

- the location of the center of area, $(x_{ca}, y_{ca}, z_{ca})_{solid}$,
- area moments of inertia, I_{cc}, I_{cn}, I_{nn}, and
- area, A_{solid}, of the cross section.

Using these available properties plus additional user-defined material properties, the required properties of the beam can be derived.

We assume that each cross section of the beam has (1) a thin-walled outer shell of constant thickness, t, (2) constant material structural properties (Young's modulus E and shear modulus G), and (3) constant shell and solid densities. Although constant everywhere in the cross section, these properties may still vary along the length of the beam as defined by the user. We assemble the components of the stiffness matrix (Eq. 1) as follows:

$$\begin{aligned} (EI)_{cc} &= Et\bar{I}_{cc} \\ (EI)_{nn} &= Et\bar{I}_{nn} \\ (EI)_{cn} &= Et\bar{I}_{cn} \\ (GJ) &= Gt\left(\bar{I}_{cc} + \bar{I}_{nn}\right) \\ (EA) &= Etp \end{aligned} \tag{2}$$

The shear stiffness terms, GK_c and GK_n, and the twist-bend coupling terms, $(EI)_{cs}$ and $(EI)_{sn}$, are not available from OpenVSP. However, the former two terms are typically very large and the latter two are typically very small, so they are set to the program defaults:

$$\begin{aligned} (EI)_{cs} &= (EI)_{sn} = \infty \\ (EI)_{cs} &= (EI)_{sn} = 0 \end{aligned} \tag{3}$$

Additionally, it follows from the thin-walled and constant-modulus assumptions that the elastic axis, tension axis and center of gravity coincide; thus, with the constant density assumption we can use the center of area from OpenVSP to represent all three.

We can therefore prepare an ASWING model for the aircraft using the degenerate Stick model exported from OpenVSP if we augment it with a modest list of additional properties:

- the lengthwise variation of material moduli, $E(s)$ and $G(s)$ (typically constant over span),
- the lengthwise variation of shell thickness, $t(s)$,
- the lengthwise variation of density of the shell material for use in modeling structural material (typically constant over span for metallic structures), and
- the lengthwise variation of density of the solid cross section for use in modeling internal masses such as fuel or payload.

In addition, for the degenerate Point model we can specify:

- constant density which can be used to calculate the total mass of the component for use as a point mass (such as a nacelle),
- the internal pressure, P, for use in calculation of fuselage pressurization loads.

Finally, ASWING requires the sectional aerodynamic coefficients for each beam that represents a lifting surface (wing, tail, etc.). For all the analyses in this paper, aerodynamic coefficients were calculated for the wing and tails using DATCOM[11]; since the overall process is modular, alternative methods such as XFoil[12], MSES[13], or FUN2D[14] could also be substituted.

D. Post-Processing of ASWING Analysis

Following its analysis, ASWING outputs the resultant internal forces along the c, s, and n axes—F_c, F_s, and F_n—and the internal moments about each axis—M_c, M_s, and M_n—at each cross section. Since ASWING does not retain information about the full geometry of the cross sections of the beam, the stresses are not calculated by the program. However, the available cross-sectional geometries from the OpenVSP Surface model can be used by the methodology to perform a calculation of the direct stresses, σ, and shear stresses, τ, resulting from each component of force or moment[15]:

$$
\begin{aligned}
\tau_{M_s} &= \frac{M_s}{2A_{\text{solid}}} \\
\sigma_{F_s} &= \frac{F_s}{pt} \\
\sigma_{M_c} &= -\frac{M_c I_{nn} - M_n I_{cn}}{I_{cc} I_{nn} - I_{cn}^2} n \\
\sigma_{M_n} &= -\frac{M_n I_{cc} - M_c I_{cn}}{I_{cc} I_{nn} - I_{cn}^2} c \\
\tau_{F_c} &= \tau_{c_b} + \tau_{c_0} \\
\tau_{F_n} &= \tau_{n_b} + \tau_{n_0}
\end{aligned}
\tag{4}
$$

where

$$
\begin{aligned}
\tau_{c_b} &= -\frac{F_c I_{cc}}{I_{cc} I_{nn} - I_{cn}^2} t \int_0^P c \, dp \\
\tau_{n_b} &= -\frac{F_n I_{nn}}{I_{cc} I_{nn} - I_{cn}^2} t \int_0^P n \, dp \\
\tau_{c_0} &= -\frac{1}{2A_{\text{solid}}} \int_0^P \tau_{c_b} c \, dp \\
\tau_{n_0} &= -\frac{1}{2A_{\text{solid}}} \int_0^P \tau_{n_b} n \, dp
\end{aligned}
\tag{5}
$$

A separate calculation is made for the hoop stress due to pressurization:

$$
\sigma_p = \frac{PR}{t}
\tag{6}
$$

where R is the radius of the cross section[15]. This calculation is performed independently from the load cases and is not part of the ASWING analysis per se.
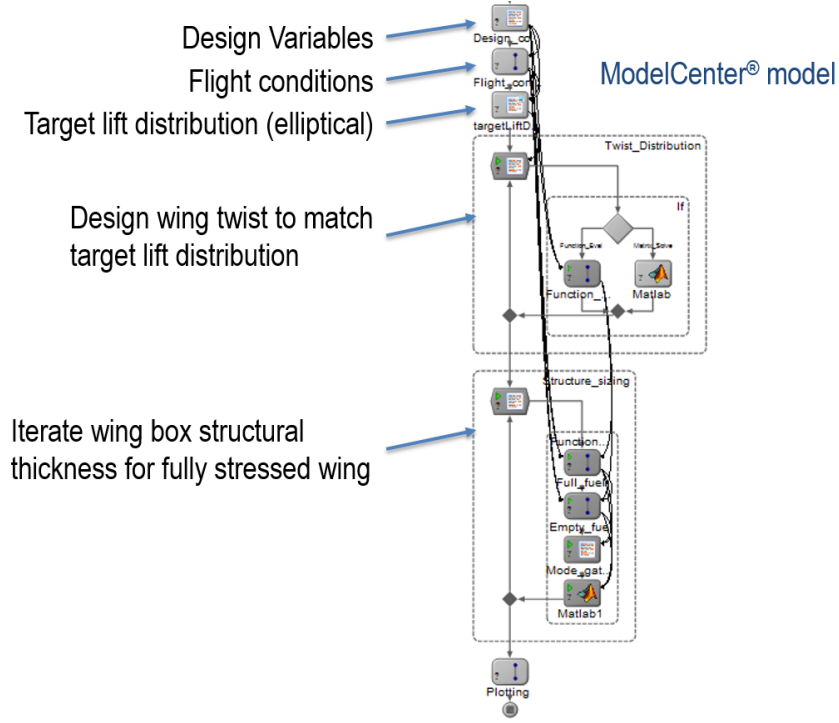
Fig. 5   Integrated analysis and sizing process

The individual components of stress can be superimposed to find the total direct and shear stresses, the maximum and minimum principal stresses, and the von Mises stress at any given location in the structure[16]:

$$\sigma_{\text{TOT}} = \sigma_{M_c} + \sigma_{F_s} + \sigma_{M_n}$$
$$\tau_{\text{TOT}} = \tau_{F_c} + \tau_{M_s} + \tau_{F_n}$$
$$\sigma_{1,2} = \frac{1}{2}\left(\sigma_{\text{TOT}} \pm \sqrt{\sigma_{\text{TOT}}^2 + 4\tau_{\text{TOT}}^2}\right) \tag{7}$$
$$\sigma_v = \sqrt{\sigma_1^2 - \sigma_1\sigma_2 + \sigma_2^2}$$

The post-processing step then finds the maximum von Mises stress over all load cases (including the separate pressurization case) for all locations on the surface, and from these values it finds the maximum von Mises stress over each entire cross section, $\sigma_{v_{\max}}$. These maximum values along the lengthwise axis are used in sizing of the structural thickness distribution, $t(s)$, as described in Section III.E.2.

E. Integrated Analysis and Sizing Process

The geometry definition and aero-structural analysis methods described in the previous sections were built into an integrated analysis and sizing process in the ModelCenter® framework[17] (Fig. 5). In addition to the analysis itself, additional scripted processes are included to design the wing twist distribution and to optimize the wing box structural thickness distribution, as described below.

1. Lift Distribution

In order to assure that the spanwise distribution of aerodynamic load on the wing is representative of the flight loads from a mature aircraft design, the twist distribution for the wing is designed to produce an elliptical lift distribution at a nominal cruise condition. The loading distribution is matched using a modal optimization process similar to that described in Ref. 18. The desired twist distribution is found using a solution of the linear system $Cx = b$, where each element C_{ij} is the change in spanwise loading coefficient at a spanwise reference station i due to a change in

twist at location j, and b_i is the residual (the difference between the desired and actual loadings) at reference station i. Therefore, x_j represents the change in twist at location j required to match the target loading distribution. To calculate the values of C_{ij}, the incidence at each cross section of the OpenVSP model is individually perturbed by a small amount (e.g. one degree) and an analysis is performed to calculate the resulting residuals to produce column j of matrix C. Typically, there are more reference stations than twist locations, and the linear system is solved using a pseudo-inverse, or least-squares, solution.

2. Structural Sizing

Once the aero-structural analysis has been performed in ASWING and the stresses are calculated in the post-processing phase, the spanwise distribution of thickness is optimized in an attempt to match the maximum von Mises stress on the surface at each cross section to the maximum allowable stress, thereby producing a fully-stressed design. An initial spanwise structural thickness distribution is chosen, and at each new iteration, $k + 1$, a new thickness is calculated at each spanwise location as follows:

$$t_{k+1} = t_k \frac{\sigma_{\text{allowable}}}{\sigma_{v_{\text{max}}}} \tag{8}$$

The thickness is subject to a minimum gauge constraint, t_{min}, and the thickness distribution is iterated until the residual is minimized.

IV. Subsonic Transport Example

The Boeing 737-200 aircraft is used in this paper as an example case to demonstrate the methodology described in Section III. This aircraft is a conventional tube-and-wing configuration and represents a technology level that is compatible with the empirical weights database used in FLOPS. Therefore, it can be expected that the FLOPS weight estimates for the aircraft are reasonably accurate. The detailed weight prediction from FLOPS for the 737-200 aircraft is given in Table 1. The weights from the FLOPS prediction were used to calibrate the sized ASWING structural model to serve as a baseline point for determination of parametric sensitivities of the weights prediction.

A. Geometry and Weights

An OpenVSP model for the aircraft is shown in Figure 6. It represents a traditional OpenVSP aircraft model with outer-moldline (OML) definitions for the fuselage, wing, tails, and nacelles, but with additional features to facilitate aero-structural analysis. First, an additional component representing the geometry of the wing torsion box was created using a wing component that is identical to the wing OML in every way, except that it is truncated at each cross section according to the chordwise fractions of the forward and rear spar. The parameters for the torsion box are linked to the wing parameters so that any change in the wing shape is automatically applied to the torsion box as well. Additional torsion boxes for the horizontal and vertical tails were created in a similar fashion. Finally, weight items with easily definable locations—such as landing gear, auxiliary power unit (APU), and control surfaces—are represented by OpenVSP "blanks" with a specified location and mass.

Other weight items were distributed throughout the aircraft as part of either the shell or solid density of the appropriate component of the model, as listed in Table 2. For each of these components, the density of the shell material and/or the solid volume of the component's Stick model was calibrated in order to match the total of the weights assigned to the component from the FLOPS prediction. Densities were held constant with span. For example, the fuselage's solid density was set such that the total integrated weight of the fuselage internal volume was equal to the weight of all items (passengers, instruments, etc.) contained within the fuselage as listed in Table 2.

As another example, the wing box's shell material density was set such that, when multiplied by the integrated volume of the shell, the weight was equal to the wing structure weight determined by FLOPS (9141 lb from Table 1). In this case, since the total volume of the shell material depends on the structural thickness distribution, this step could only be undertaken once the thickness optimization process described in Section III.E.2 was completed. The wing box's solid material density was set such that the weight of the enclosed volume was equal to the mission fuel weight.

Once this calibration process had been applied to all of the components in Table 2 and appropriate weights had been assigned to the blanks in the OpenVSP model, a fully-calibrated 737-200 model was ready for use as a baseline in the parametric analysis of Section V.

Table 1   737-200 predicted weight summary from FLOPS.

Item	Percent	Weight (lb)
Wing	7.88	9141
Horizontal Tail	1.12	1295
Vertical Tail	0.71	829
Fuselage	10.56	12246
Landing Gear	3.78	4383
Nacelle (Air Induction)	0.49	574
Structure Total	24.54	28468
Engines	5.51	6392
Miscellaneous Systems	0.19	219
Fuel System–Tanks and Plumbing	0.48	553
Propulsion Total	6.18	7164
Surface Controls	1.11	1293
Auxiliary Power	0.78	902
Instruments	0.36	420
Hydraulics	0.71	826
Electrical	1.46	1699
Avionics	1.02	1188
Furnishings and Equipment	9.29	10780
Air Conditioning	1.20	1390
Anti-Icing	0.13	148
Systems and Equipment Total	16.07	18644
Weight Empty	46.79	54276
Crew and Baggage–Flight, 2	0.39	450
Crew and Baggage–Cabin, 4	0.53	620
Unusable Fuel	0.37	429
Engine Oil	0.07	83
Passenger Service	1.83	2118
Cargo Containers	0.91	1050
Operating Weight	50.88	59026
Passengers, 136	19.34	22440
Passenger Baggage	4.69	5440
Zero Fuel Weight	74.92	86906
Mission Fuel	25.08	29094
Ramp (Gross) Weight	100.00	116000

Fig. 6   737-200 OpenVSP model

Table 2   Distribution of additional weight components

Component	Weight Items Included
Wing box shell	Wing structure
Horizontal tail box shell	Horizontal tail structure
Vertical tail box shell	Vertical tail structure
Fuselage shell	Fuselage structure
Wing box solid	Mission fuel, tanks & plumbing, hydraulics, anti-ice, unusable fuel
Fuselage solid	Passengers, instruments, electrical, avionics, air conditioning, crew, baggage, passenger service, cargo containers, cargo
Nacelle solid	Engines, thrust reversers, engine oil

Table 3   Load cases used for structural sizing

Name	Load Factor	Sideslip (°)	Horiz. Tail (°)	Elev. (°)	Rudder (°)	Aileron (°)	Thrust	Roll Rate (°/s)	Pitch Rate (°/s)	Vert. Accel. (g)
Cruise	1		trim				trim			
2.5-g Pull-up	2.5		trim				trim			
1.0-g Pushover	-1		trim				trim			
Taxi bump										2
Dyn. over-swing	1	5	trim		-27	trim	trim			
Rudder reversal	1	5	trim		27	trim	trim			
Initial roll+	1		trim		trim	-20	trim			
Initial roll-	1		trim		trim	20	trim			
Checked roll+	1		trim		trim	20	trim	5		
Checked roll-	1		trim		trim	-20	trim	5		
Initial pitch+	1			-17			trim			
Initial pitch-	1			17			trim			
Checked pitch+	1			17			trim		5	
Checked pitch-	1			-17			trim		5	

B. Load Cases

The load cases used for sizing of the thickness distributions of all beams are shown in Table 3; blank entries indicate values of zero. The first four load cases (cruise, 2.5-g pull-up, 1.0-g push-over, and taxi bump) were used throughout the study to size the structure as the wing shape was changed, while the rest of the load cases in the table were only used initially to size the fuselage and tail surfaces. In all but the taxi bump case, one or more of the control surfaces were used to trim the flight condition; for example, in the cruise case the horizontal tail incidence angle was used to trim for zero pitch acceleration, while the engine thrust was used to trim for zero longitudinal acceleration. In addition, all load cases were run with the wing both full of fuel and empty.

ASWING also has the ability to factor in additional load cases that were not used here. Additional load cases, such as crash loads, dynamic taxi bump simulation, and dynamic gust loads could prove to be important to certain highly-flexible aircraft configurations.

C. Sizing Results

The wing, fuselage, and tail structural thickness distributions were sized according to the process described in Section III.E.2. An allowable stress of 3.74×10^6 psf was used, which was derived from a nominal yield strength for aluminum of 5.62×10^6 psf and a factor of safety of 1.5. A minimum gauge constraint of 0.01 ft was also used.

The sized structural thickness distribution and the resulting distribution of maximum von Mises stress for the wing are shown in Fig. 7. The stress distribution is closely matched to the allowable stress from the root to about 75% of the span. Outboard of this location, the thickness is constrained by the minimum gauge; as the aerodynamic loading drops to zero at the tip, the maximum stress also drops to zero and the wing box is thicker than it needs to be based on allowable stress.

Figure 8 shows the maximum von Mises stress over all of the wing sizing loading cases (rows 1–4 of Table 3), including the separate fuselage pressurization case. The stress is equal to the allowable, or nearly so, for much of the wing box and fuselage surfaces. The stress on the fuselage surface reaches a maximum in regions of maximum radius. The stresses on the tails are less than the allowable because the thicknesses of those components were sized based on the additional load cases not included in the analysis results shown in the figure.

As seen previously in Fig. 7, the maximum wing stress is equal to the allowable stress inboard of 75% span, and drops to zero at the tip. However, at each inboard cross section, the stress is equal to the allowable at only one location and is less than the allowable at other points in the cross section. Since the simplified model is limited to a constant
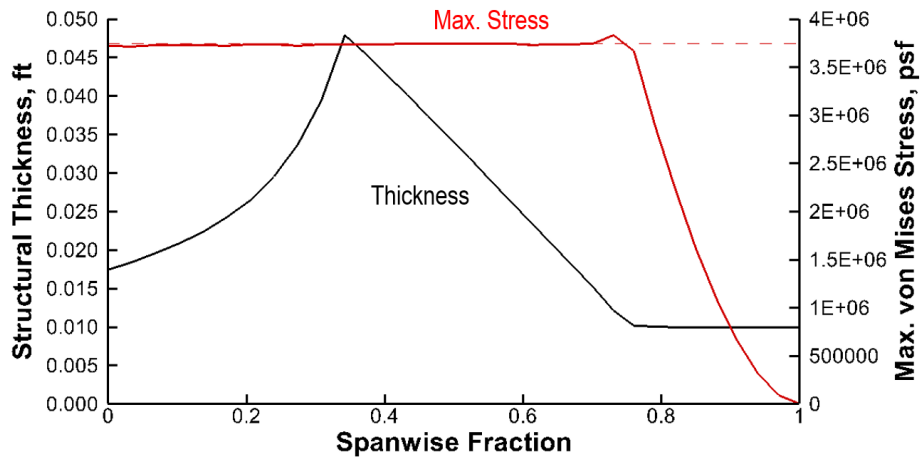
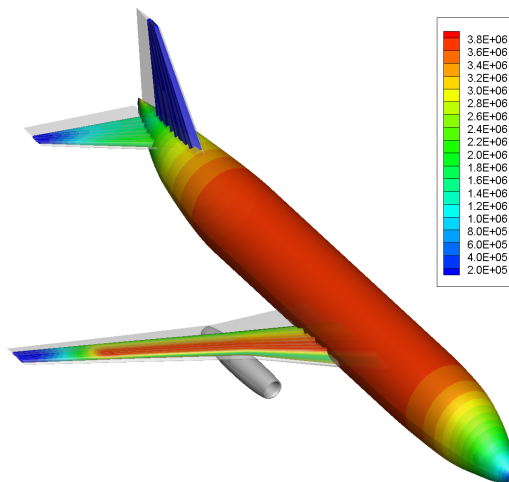**Fig. 7   737-200 sized wing-box thickness distribution and maximum sectional stresses**

Fig. 8   737-200 maximum von Mises stresses over all primary load cases
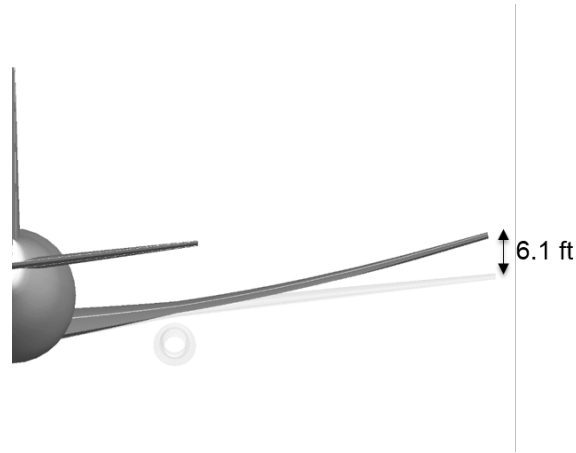
13

Fig. 9   737-200 wing deflection for a 2.5-g pull-up maneuver

thickness everywhere in the cross section, most of the cross section is actually thicker than required and the complete three-dimensional structure is not actually a fully-stressed design.

Finally, Fig. 9 shows the wing deflection for the 2.5-g pull-up maneuver. For this class of aircraft, one might expect the tip deflection to be significantly higher at this high-load condition. However, as discussed above, due to the simplifications in the structural model, the structure is somewhat thicker than required in many locations, and consequently can be expected to be stiffer than a model with more design variables. If a more accurate prediction of wing tip deflection were required—for example, if wing tip strike during taxi bump were a concern for a very-high-aspect-ratio wing—then the flexibility of the model could be increased by artificially increasing the allowable stress to compensate.

Alternatively, the complexity of the model could be increased by allowing the structural thickness to vary at different points along the cross section—for example, defining separate thicknesses for the forward and aft spars and the upper and lower skins–at the expense of increased complexity in model setup. A non-constant thickness at the cross section would mean that the constant-thickness moments of inertia from OpenVSP could no longer be used, and a full calculation of the stiffness properties would be required during preparation of the ASWING model using numerical integration.

V. Parametric Analysis

A. Parametric Study Setup

Once the baseline 737-200 aero-structural model was calibrated, a parametric study was performed by varying certain wing planform design variables relative to their baseline values. This parametric variation was performed in two stages:

- First, a two-level full-factorial design of experiments (DOE) was performed to test all combinations of variables at their minimums and maximums. By testing the model at the corners of the design space, it was possible to test the robustness of the model and to assess the sensitivity of the wing weight to variations in each of the design variables.
- Finally, a central-composite DOE was performed to develop a non-linear surrogate model relating the wing weight to values of the wing planform design variables.

The design variables and their ranges are shown in Table 4. These variables were chosen because they represent the most influential planform variables in the FLOPS weight equations. Since the thickness/chord ratio varies by cross section, a single thickness/chord factor was defined as a multiplier on the thickness/chord ratios of all sections.

B. Wing Weight Trends

Using the analysis results from the central-composite DOE, kriging was used to create a surrogate model that relates the wing weight to the values of the chosen design variables. Figure 10 compares actual vs. predicted values of wing weight for all combinations of design variables in the DOE matrix. The approximation error is reasonable throughout the design space, and the model has a statistical $R^2 = 0.9985$, indicating high reliability in reproducing the weights in

Table 4   Design variables and ranges for parametric variation

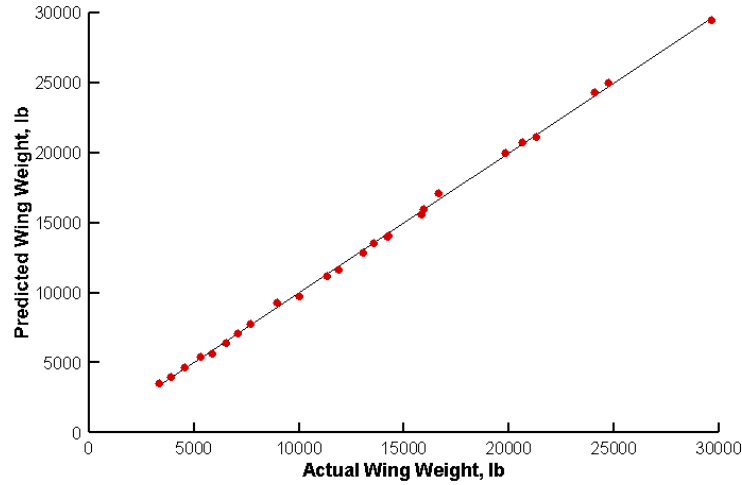| Variable	Minimum	Maximum
Wing area, ft^2	600	1600
Aspect ratio	6	17
Thickness/chord factor	0.8	1.2
Fuel weight, lb	15,000	45,000

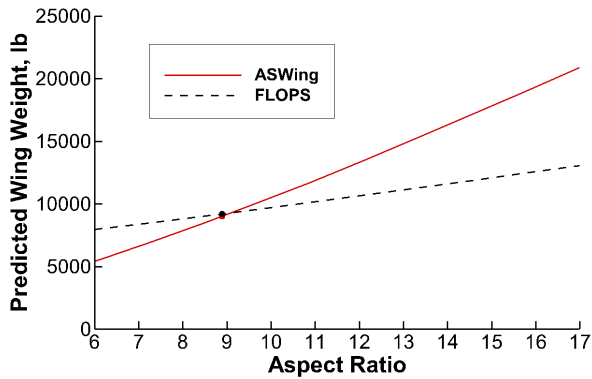**Fig. 10   Actual vs. predicted wing weight for points in the design matrix**

the DOE matrix.

Figure 11 compares the wing-weight trends derived from the aero-structural sizing methodology to similar calculations using the existing weight equations in FLOPS. For all design variables, the aero-structural methodology shows the expected trends (i.e., wing weight increases with increased wing area and fuel weight and decreases with increasing thickness/chord ratio). For the wing area, thickness/chord ratio, and fuel weight, the trends track the FLOPS trends closely. However, the aero-structural methodology shows much more sensitivity of wing weight to aspect ratio than FLOPS does. It has been the experience of multiple users, though not fully documented, that FLOPS lacks proper sensitivity to aspect ratio as it is increased beyond the bounds of its original database; therefore, it is very possible that the increased sensitivity of the aero-structural methodology represents a more accurate prediction than FLOPS.
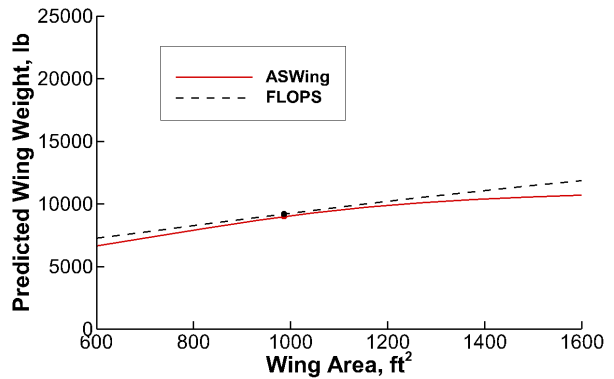
As explained in Section III.E.2, the structural thickness of the wing box is constrained by a minimum gauge value. Since the structural model is somewhat abstract and not a detailed representation of the true internal geometry, the choice of an appropriate minimum gauge is not readily obvious. As a result, the original choice of $t_{min} = 0.01$ ft was somewhat arbitrary. In an attempt to understand the importance of the choice of minimum gauge on the weight trends, the DOE was repeated with an alternative choice of $t_{min} = 0.02$ ft. Figure 12 compares the wing-weight trends with respect to aspect ratio and wing area, for the two different values of minimum gauge. The choice of a larger minimum gauge results in an increase in wing weight at lower aspect ratios and larger wing areas. These are regions of the design space where the structural design is less challenging, so that more of the wing span would be sized with a small thickness value if it were not for the minimum gauge constraint. The increased value of t_{min} brings the results from the aero-structural methodology more in line with FLOPS at lower aspect ratios, which is the region where FLOPS can be expected to be accurate, giving evidence that the larger minimum gauge is a more appropriate choice.
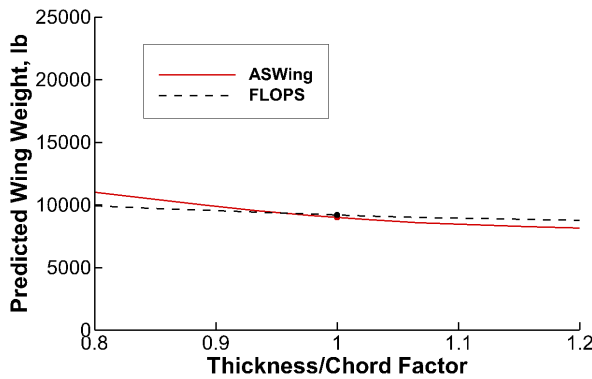
VI. Conclusion

In this study, an integrated aero-structural analysis and sizing methodology was developed which leverages the equivalent-beam properties automatically exported from OpenVSP in order to easily integrate the geometry definition
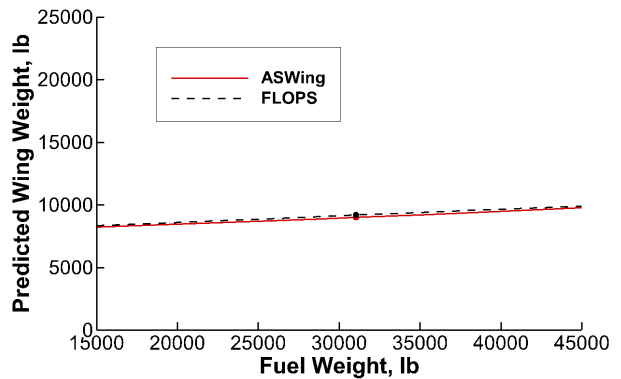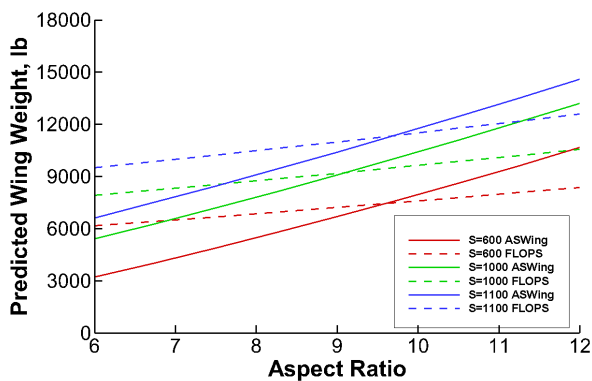
(a) aspect ratio

(b) wing area
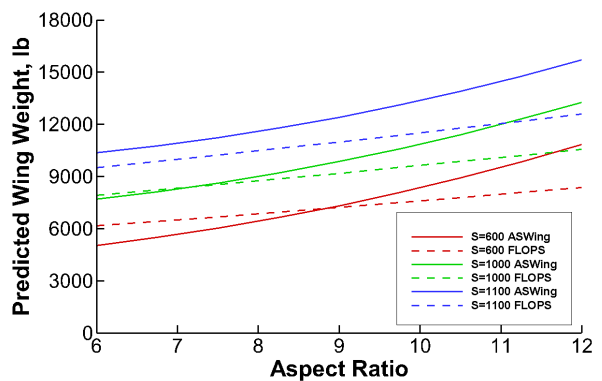
(c) thickness/chord factor

(d) fuel weight

Fig. 11 Wing-weight trends with respect to wing planform design parameters, $t_{\mathbf{min}} = 0.01$ ft

(a) $t_{\mathrm{min}} = 0.01$ ft

(b) $t_{\mathrm{min}} = 0.02$ ft

Fig. 12 Effect of minimum gauge constraint on wing-weight trends

16

with the aero-structural analysis in ASWING. The integrated process builds upon an existing multi-disciplinary process that leverages the DegenGeom geometry forms in OpenVSP. First, an analytical model of the Boeing 737-200 was built and calibrated to the empirical weights predictions from FLOPS. Next, the baseline 737-200 model was used as a point of departure to assess the sensitivity of wing weight to certain planform design variables.

Whereas a single prediction of the full aircraft weight breakdown in FLOPS might take approximately 1 second to execute on a laptop computer, an analysis in ASWing might take approximately 1–2 seconds per load case. Combined with the need for multiple load cases, a wing spanwise loading optimization loop, and a structural thickness optimization loop, as well as computational overhead from the ModelCenter environment, a full weight prediction in the new methodology was found to require up to 1–2 minutes. This is an order of magnitude longer than the FLOPS analysis, but is still much less time than a FEM-based prediction, which could be expected to take several hours to complete the structural sizing process. Therefore, the methodology is able to fill a middle ground between an empirical prediction in FLOPS and a higher-order FEM-based sizing process. Furthermore, once the results of the parametric analysis have been used to create a surrogate model for the wing weight, then the surrogate can be executed with minimal computational cost for subsequent design studies.

The parametric wing-weight trends from the physics-based process are consistent with expected trends (e.g., wing weight increases monotonically with aspect ratio). While the trends are similar to FLOPS for most wing parameter variables, the wing weight was found to be more sensitive to aspect ratio than FLOPS. This gives preliminary indications that the low-order methodology offers improved fidelity compared to FLOPS, but further validation will be required to reach a firm conclusion. Also, the wing-weight trends were found to be sensitive to the choice of minimum gauge, so further studies should be conducted to help in choosing appropriate values for this constraint.

For the 737-200 model, the predicted tip deflection at high load factors appears to be smaller than the true expected deflection; this under-prediction is likely due in part to the assumption of constant cross-sectional structural thickness, which results in a surface that is not fully-stressed at all potential points. For applications where wing tip deflections are a potential constraint, it might be possible to increase the accuracy of the predicted deflection by artificially increasing the allowable stress to compensate. It also could be useful to examine the use of a more general sizing methodology that uses separate thicknesses for front/rear spars, upper/lower skins and compare the results to the constant-thickness assumption.

In this study, a conventional tube-and-wing aircraft configuration was analyzed in order to benchmark the results for a configuration for which FLOPS weights estimates are expected to be reliable. However, an advantage of replacing empirical methods with more physics-based analysis is that it is likely to increase the validity of the analysis for unconventional configurations and advanced materials. It will be useful to conduct further studies on the applicability of this methodology to configurations such as a hybrid wing-body, supersonic configuration, or truss-braced wing.

Finally, it will be useful to extend the sizing methodology to include a method for analyzing flutter and estimating the weight penalty associated with meeting the required flutter margin. This additional capability would improve the sizing of very-high-aspect-ratio wings for which flutter is an important constraint. ASWING has the capability to perform flutter analysis, both as modal and time-domain solutions, so adding in these capabilities would only require modest changes to the model generation. One important step would be to include the bending-torsion coupling terms, $(EI)_{cs}$ and $(EI)_{sn}$, in the stiffness matrix of Eq. 1; since these terms are not calculated as part of the OpenVSP degenerate geometry model generation, inclusion of these terms would require additional preprocessing using shear-flow analysis.

Acknowledgments

References

[1] Raymer, D. P., *Aircraft Design: A Conceptual Approach*, AIAA Education Series, Washington, DC, 1989.

[2] Wells, D. P., Horvath, B. L., and McCullers, L. A., "The Flight Optimization System Weights Estimation Method," NASA TM–2017–219627, 2017.

[3] Nickol, C. L., and McCullers, L. A., "Hybrid Wing Body Configuration System Studies," *47th AIAA Aerospace Sciences Meeting Including The New Horizons Forum and Aerospace Exposition*, AIAA 2009–931, Orlando, FL, 2009. doi:10.2514/6.2009-931.

[4] Hahn, A., "Vehicle Sketch Pad: A Parametric Geometry Modeler for Conceptual Aircraft Design," *48th AIAA Aerospace Sciences Meeting Including the New Horizons Forum and Aerospace Exposition*, AIAA 2010–657, Orlando, FL, 2010. doi:10.2514/6.2010-657.

[5] Ordaz, I., "Conversion of Component-Based Point Definition to VSP Model and Higher-Order Meshing," *49th AIAA Aerospace Sciences Meeting Including the New Horizons Forum and Aerospace Exposition*, AIAA 2011–358, Orlando, FL, 2011. doi:10.2514/6.2011-358.

[6] Chaput, A., and Rizo-Patron, S., "Vehicle Sketch Pad Structural Analysis Module Enhancements for Wing Design," *50th AIAA Aerospace Sciences Meeting Including the New Horizons Forum and Aerospace Exposition*, AIAA 2012–0546, Nashville, TN, 2012. doi:10.2514/6.2012-546.

[7] Hahn, A., "Application of Cart3D to Complex Propulsion-Airframe Integration with Vehicle Sketch Pad," *50th AIAA Aerospace Sciences Meeting Including the New Horizons Forum and Aerospace Exposition*, AIAA 2012–0547, Nashville, TN, 2012. doi:10.2514/6.2012-547.

[8] Belben, J. B., and McDonald, R. A., "Enabling Rapid Conceptual Design Using Geometry-Based Multi-Fidelity Models in VSP," *51st AIAA Aerospace Sciences Meeting Including the New Horizons Forum and Aerospace Exposition*, AIAA 2013–0328, Grapevine, TX, 2013. doi:10.2514/6.2013-328.

[9] Olson, E. D., "Multi-Disciplinary, Multi-Fidelity Discrete Data Transfer Using Degenerate Geometry Forms," *17th AIAA/ISSMO Multidisciplinary Analysis and Optimization Conference*, AIAA 2016–3208, Washington, DC, 2016. doi:10.2514/6.2016-3208.

[10] Drela, M., *ASWING 5.99 Technical Description—Steady Formulation*, MIT Department of Aeronautics and Astronautics, 2015.

[11] "USAF Stability and Control DATCOM," ADB072483, Wright-Patterson Air Force Base, Ohio, 1976.

[12] *XFoil, Software Package, Ver. 6.97*, Massachusetts Institute of Technology, Cambridge, MA, 2008.

[13] *MSES, Software Package, Ver. 3.08*, Massachusetts Institute of Technology, Cambridge, MA, 2008.

[14] Biedron, R. T., et al., "FUN3D Manual: 13.2," NASA TM–2017–219661, 2017.

[15] Megson, T. H. G., *Aircraft Structures for Engineering Students*, 5th ed., Elsevier, Boston, 2013.

[16] Dowling, N. E., *Mechanical Behavior of Materials: Engineering Methods for Deformation, Fracture, and Fatigue*, 4th ed., Pearson Education, London, 2012.

[17] *ModelCenter, Software Package, Ver. 11.2*, Phoenix Integration, Blacksburg, VA, 2015.

[18] Lane, K. A., Marshall, D. D., and McDonald, R. A., "Lift Superposition and Aerodynamic Twist Optimization for Achieving Desired Lift Distributions," *48th AIAA Aerospace Sciences Meeting Including the New Horizons Forum and Aerospace Exposition*, AIAA 2010–1227, Orlando, FL, 2010. doi:10.2514/6.2010-1227.